

## Mineral reactions at a peridotite-gneiss contact, Jotunheimen, Norway<sup>1</sup>

W. L. GRIFFIN<sup>2</sup>

Mineralogisk-Geologisk Museum, Oslo

**SUMMARY.** The assemblage aluminous pyroxenes + spinel forms reaction zones between olivine-rich and plagioclase-rich layers in the Jotunheimen complex. These zones have probably formed by cooling from high  $T$  at moderate  $P$ , passing through the  $ol + plag \rightarrow pyroxenes + spinel$  reaction. The absence of garnet, which would be expected to form upon further cooling, is attributed to interruption of the cooling history by rapid uplift. This uplift is demonstrated by symplectitic breakdown of aluminous pyroxenes, with expulsion of  $Ts$  and  $Acm$ , to yield low-Al pyroxenes, spinel, and plagioclase. The uplift must be Precambrian, and suggests that the Jotun rocks were involved in rapid vertical movements long before the Caledonian thrusting took place.

**ROCKS** of the Bergen-Jotun kindred (Goldschmidt, 1916), ranging from peridotites and anorthosites to mangerites, crop out over large areas in Jotunheimen, central Norway. These occurrences, and others extending over 150 km to the SSW, make up the Jotun nappe of the Caledonian mountain chain (fig. 1). The movement plane separating the Jotun crystalline rocks from the younger underlying sediments dips steeply under the nappe on the northern border, but is gently dipping to nearly flat-lying along the southern margin, where deep valleys cut completely through the crystalline rocks. It is generally agreed that thrusting has taken place along the borders of the massif in Caledonian time, but the distance of movement and the location of the root zone are matters of considerable debate. A summary of the geology and of geophysical data bearing on the shape of the Jotun nappe are given by Smithson and Ramberg (1970).

A nappe origin has also been suggested for the occurrences of Jotun-type rocks in the Bergen area (Kvale, 1960), but the field relations are less definite.

Batthey (1960) described the peridotites that occur as conformable sheets in the pyroxene gneisses of the High Jotunheim, and concluded that an intrusive origin was possible for the peridotites. Further work, however, indicated that the gneisses and the peridotites are members of a large layered complex, possibly lopolithic in form (Batthey, 1965). Although an igneous origin for the complex seems certain, Batthey (1960) has drawn attention to the fact that the rocks in their present state are metamorphic, with granulite-facies mineral assemblages. This is demonstrated not only by their fabrics, but by the presence of complex spinel-bearing reaction zones at the peridotite-gneiss contacts (see fig. 2 in Batthey, 1960). Most such zones are amphibolitized and their detailed interpretation is not obvious. We describe here a relatively

<sup>1</sup> Publication no. 27 in the Norwegian Geotraverse Project.

<sup>2</sup> Present address: Institut for Geologi, Blindern, Oslo.

anhydrous example, and attempt to correlate its mineralogy with appropriate experimental studies.

Corona structures (reaction rims) between olivine and plagioclase have been used previously (Griffin, 1971*a, b*) to study the thermal and tectonic history of anorthositic rocks from the western part of the Upper Jotun nappe and from the Bergen Arcs (fig. 1). The reaction zone described here represents an earlier stage of corona evolution than is preserved in those areas.

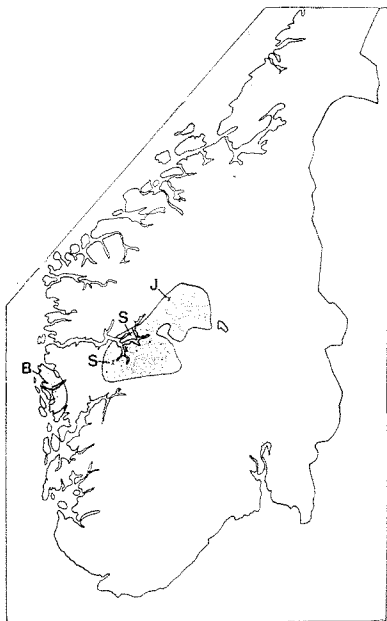


FIG. 1. Southern Norway, showing extent of the Upper Jotun Nappe and of similar rocks in the Bergen Arcs (B). S, Sognefjord areas discussed by Griffin (1971*a*); J, locations of samples discussed in this paper.

*Location.* The contact reaction zone described here (Sample J/58/63)<sup>1</sup> was collected about 2.5 km on 32° bearing from Spiterstulen hotel, Visdalen, in the small area figured by Battey (1960, fig. 2). Gneiss sample JS23 was collected about 2 km on 55° bearing from Spiterstulen hotel.

*Chemical data.* Some reaction zones and symplectites may be compared with experimental studies to deduce part of the *P-T* history of the rock, provided we have detailed compositional data on the reactants and the products of the presumed reaction. In this study a combination of textural observations and microprobe analysis has been used to deduce the reactions involved. Microprobe analyses of the minerals are presented in tables I and II. Analytical methods have been described by Griffin (1971*a, b*).

The reactions involving pyroxenes are most easily discussed in terms of normative components, but calculation of structural formulae and of these components requires knowledge of the  $\text{Fe}_2\text{O}_3/\text{FeO}$  ratio, which is not obtained from microprobe analysis. The  $\text{Fe}_2\text{O}_3/\text{FeO}$  ratio and normative pyroxene components have therefore been calculated in the following manner, which assumes that the pyroxenes are stoichiometric: the structural formula to 6 oxygens is calculated assuming no  $\text{Fe}_2\text{O}_3$ . Ti is assigned to  $\text{CaTiAl}_2\text{O}_6$  and the equivalent amount of  $\text{Al}^{\text{IV}}$  subtracted. Tschermak's molecule ( $\text{CaAl}_2\text{SiO}_6$ ) is taken as equal to  $\text{Al}^{\text{VI}}$ . In all of the pyroxenes discussed here,  $\text{Al}^{\text{IV}} > \text{Al}^{\text{VI}}$  already at this stage of the calculation, indicating that jadeite ( $\text{NaAlSi}_2\text{O}_6$ ) is absent and all Na is present as acmite ( $\text{NaFe}^{3+}\text{Si}_2\text{O}_6$ ). To balance the structural formula it was assumed that the  $\text{Al}^{\text{IV}}$  in excess of  $(2\text{Ti} + \text{Al}^{\text{VI}})$  is balanced by  $\text{Fe}^{3+}$  in the octahedral sites, i.e. that a  $\text{CaFe}^{3+}\text{AlSiO}_6$  member is present. Fe is divided accordingly and the calculation reiterated until no further change in  $\text{Fe}_2\text{O}_3$  is possible at the 0.1 wt % level. In the final normative calculations the end members are calculated in the order  $\text{CaTiAl}_2\text{O}_6$ , Acm, Ts,  $\text{CaFe}^{3+}\text{AlSiO}_6$ , Di+Hd,  $(\text{Mg,Fe})_2\text{Si}_2\text{O}_6$ .

<sup>1</sup> Numbers refer to samples in collections at the University of Newcastle upon Tyne.

Hornblende structural formulae are calculated to the anhydrous basis of 23 oxygens, taking all Fe as FeO. Spinel formulae are calculated to 32 oxygens; the imbalance of the formulae shows that some of the iron is present as Fe<sub>2</sub>O<sub>3</sub>.

*Description.* The general sequence of phases in the contact zone is peridotite (oliv+cpx+hbl)—opx+spinel zone—cpx+spinel zone—cpx+spinel+plag gneiss. Microprobe analyses of the phases are given in table I.

TABLE I. *Microbe analyses of phases in contact sample J58/63*

	Peridotite			Reaction zone			Gneiss		Symplectite in gneiss	
	oliv	cpx	hbl	spin	opx	cpx	cpx	spin	opx	cpx
SiO <sub>2</sub>	39.4	50.4	39.6	0.0	53.7	50.3	48.9	0.0	51.9	49.4
TiO <sub>2</sub>	0.0	0.2	1.2	0.0	0.1	0.3	0.6	0.0	0.0	0.5
Al <sub>2</sub> O <sub>3</sub>	—	5.3	14.2	64.0	3.3	5.1	8.1	61.7	2.4	5.5
Fe <sub>2</sub> O <sub>3</sub>	—	4.7	—	—	—	4.6	5.9	—	—	4.9
FeO	20.4	2.1	9.0	23.1	13.6	2.3	1.5	30.2	21.1	2.6
MgO	39.9	15.2	14.8	12.5	28.8	15.1	12.9	8.3	23.6	14.6
CaO	—	21.6	13.5	0.0	0.3	21.5	20.1	0.0	0.5	21.3
Na <sub>2</sub> O	—	0.8	2.7	—	—	0.8	1.9	—	—	0.8
K <sub>2</sub> O	—	0.0	1.2	—	—	0.0	0.0	—	—	0.0
Sum	99.7	100.2	96.2	99.6	99.8	100.0	99.9	100.2	99.5	99.6
Si	0.988	1.843	5.932	—	1.918	1.846	1.794	—	1.929	1.826
Al <sup>iv</sup>	—	0.157	2.068	15.975	0.082	0.154	0.206	15.862	0.071	0.174
Al <sup>vi</sup>	—	0.072	0.439	—	0.057	0.067	0.144	—	0.034	0.066
Ti	—	0.006	0.135	—	0.003	0.008	0.017	—	—	0.014
Fe <sup>3+</sup>	—	0.130	—	—	—	0.127	0.163	—	—	0.136
Fe <sup>2+</sup>	0.451	0.064	1.127	4.091	0.406	0.071	0.046	5.509	0.656	0.080
Mg	1.573	0.829	3.305	3.946	1.533	0.826	0.706	2.698	1.308	0.805
Ca	—	0.846	2.167	—	0.011	0.845	0.790	—	0.020	0.844
Na	—	0.057	0.784	—	—	0.057	0.135	—	—	0.057
K	—	—	0.229	—	—	—	—	—	—	—
<b>Pyroxene components:</b>										
CaTiAl <sub>2</sub> O <sub>6</sub>		0.6			0.8	1.7				1.4
NaFeSi <sub>3</sub> O <sub>6</sub>		5.7			5.7	13.5				5.7
CaAl <sub>2</sub> SiO <sub>6</sub>		7.2			6.7	14.4				6.6
CaFeAlSiO <sub>6</sub>		7.3			7.0	2.8				7.9
Ca(Fe,Mg)Si <sub>2</sub> O <sub>6</sub>		69.5			70.0	60.1				68.5
(Fe,Mg) <sub>2</sub> Si <sub>2</sub> O <sub>6</sub>		19.9			19.8	7.5				10.0
		100.2			100.0	100.0				100.1

The peridotite consists dominantly of coarse-grained (2 mm) olivine with minor interstitial clinopyroxene and amphibole of similar grain size. No orthopyroxene was observed within the peridotite proper in this specimen. The olivine is granulated along grain boundaries, but strain is not especially pronounced within the large grains. Thin bands of fine-grained opaques cut the large grains but do not appear related to serpentinization, which is very light. Analyses of many olivine grains from different parts of the band show little variation from Fo<sub>77</sub>. The clinopyroxenes are identical

in composition to those in the corona (see below); the moderate Al content is present entirely as the Tschermak's component ( $\text{Ca}(\text{Fe}, \text{Al})_2\text{SiO}_6$ ). Many of the clinopyroxene grains contain trains of exsolved spinel grains, and locally break down into orthopyroxene-plagioclase-spinel symplectites.

The orthopyroxene zone is a mixture of orthopyroxene, minor clinopyroxene, and abundant spinel in 1 to 2 mm grains. Orthopyroxene ( $\text{En}_{79}$ ) is strongly pleochroic in pink and red-brown and contains wedge-shaped clinopyroxene lamellae; some large grains show mechanical deformation, with kinking of the exsolution lamellae. The spinel forms dark green anhedral grains interstitial to the orthopyroxene; much of the spinel is altered irregularly to an almost opaque mixture of green spinel and finely divided magnetite. Pyroxene-plagioclase symplectites are developed at pyroxene grain boundaries, within pyroxene grains as patches or bands, and at orthopyroxene-spinel contacts.

The clinopyroxene zone is finer grained (0.5–1 mm) and contains abundant spinel, minor orthopyroxene, and local corroded relicts of olivine. The clinopyroxene is full of orthopyroxene lamellae and somewhat pigmented. It is nearly identical in composition to the pyroxene within the olivine band. Orthopyroxene-plagioclase-spinel symplectite, with minor clinopyroxene, is extensively developed along pyroxene-pyroxene and pyroxene-spinel boundaries, and within individual clinopyroxene grains. These symplectites are locally replaced by dark brown poorly crystallized hornblende, especially toward the outer part of the zone.

The gneiss is equigranular but has a foliation defined mainly by trains of clinopyroxene (0.5–1 mm) and spinel ( $< 0.5$  mm). The clinopyroxene is more acmitic and Tschermakitic than that in the corona; the spinel is more iron-rich and has higher  $\text{Fe}^{3+}/\text{Fe}^{2+}$ . Much of the clinopyroxene is decomposed to two-pyroxene-plagioclase symplectites, and pseudomorphs of symplectite after clinopyroxene grains are abundant. As shown in table I, the symplectite pyroxene contains less Al and less Na than the primary pyroxene. The spinel grains are corroded, nearly opaque in most cases, and are typically separated from the clinopyroxene by plagioclase collars. The plagioclase grains ( $\sim 0.5$  mm) are strongly zoned, from about  $\text{An}_{35}$  in the cores to  $\text{An}_{60-65}$  at the rims. The plagioclase in the symplectites is  $\text{An}_{67}$ , and it seems clear that the zoning is related to the pyroxene breakdown. Brown hornblende, similar to that in the corona, replaces the symplectite widely, and biotite is apparently also secondary.

The gneiss JS23 also is weakly foliated, and consists largely of mesoperthite, clinopyroxene, and plagioclase. Plagioclase is confined almost completely to rings around corroded pyroxene grains (fig. 2). Scattered within this relatively homogeneous plagioclase ( $\text{An}_{41-44}$ ) are small granules of clinopyroxene, orthopyroxene ( $\text{En}_{62}$ ), and magnetite, as well as some biotite flakes. The pyroxenes, which are similar to those in the gneiss of sample 58/63, are full of parallel lamellae of plagioclase ( $\text{An}_{43}$ ) and magnetite. It seems clear from the textures that the plagioclase, the magnetite, and the pyroxene granules (table II) are the products of pyroxene breakdown. This texture is common in the pyroxene/mesoperthite gneisses of the area.

In other gneisses near to the peridotite bodies in the area from which JS23 comes, small amounts of garnet may be present. The characteristic occurrence in unaltered

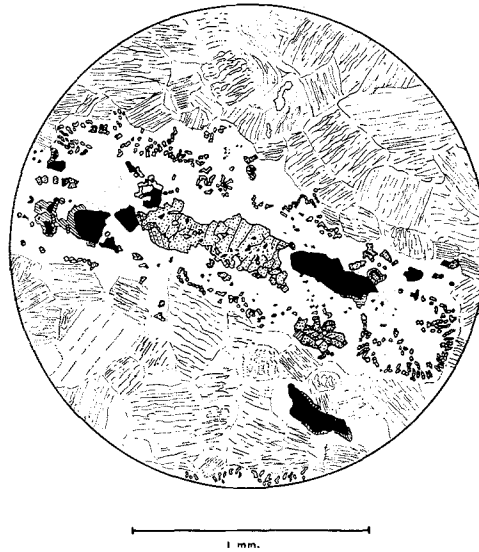


FIG. 2. Gneiss JS23, showing corroded pyroxene surrounded by a ring of homogeneous plagioclase, sprinkled with granules of opx, cpx, and mgt (partly rimmed by biotite). The field outside the corona structure is of mesoperthite. Drawing from a photo-micrograph.

TABLE II. *Pyroxene analyses, gneiss JS23*

	cpx cores	cpx rims	cpx granules	opx granules		cpx cores	cpx rims	cpx granules	opx granules
SiO <sub>2</sub>	49.7	51.7	52.4	51.6	Si	1.852	1.921	1.951	1.967
TiO <sub>2</sub>	0.5	0.4	0.2	0.0	Al <sup>iv</sup>	0.148	0.079	0.049	0.032
Al <sub>2</sub> O <sub>3</sub>	5.1	2.8	1.8	1.0	Al <sup>vi</sup>	0.076	0.044	0.030	0.013
Fe <sub>2</sub> O <sub>3</sub>	3.6	2.2	1.5	—	Ti	0.014	0.011	0.006	—
FeO	6.3	6.1	6.8	23.8	Fe <sup>3+</sup>	0.101	0.062	0.042	—
MgO	12.9	14.3	14.6	21.6	Fe <sup>2+</sup>	0.196	0.189	0.212	0.759
CaO	21.0	21.4	21.7	0.3	Mg	0.717	0.792	0.810	1.227
Na <sub>2</sub> O	0.8	0.7	0.5	—	Ca	0.839	0.852	0.865	0.012
	99.9	99.6	99.5	98.3	Na	0.058	0.050	0.036	—
					CaTiAl <sub>2</sub> O <sub>6</sub>	1.4	1.1	0.6	
					NaFeSi <sub>2</sub> O <sub>6</sub>	5.8	5.0	3.6	
					CaAl <sub>2</sub> SiO <sub>6</sub>	7.6	4.4	3.0	
					CaFeAlSiO <sub>6</sub>	4.3	1.2	0.6	
					Ca(Fe,Mg)Si <sub>2</sub> O <sub>6</sub>	70.6	78.5	82.3	
					(Fe,Mg) <sub>2</sub> Si <sub>2</sub> O <sub>6</sub>	10.3	9.8	9.9	
						100.1	100.0	100.0	

granulites is as a thin pellicle, along with biotite, around amoeboid magnetite grains. With the onset of amphibolitization of pyroxene, garnet becomes more abundant, and forms euhedral grains, which commonly appear to replace biotite. The paragenesis is similar to some described by Griffin and Heier (1969) in retrograded granulites from Lofoten and appears to be a retrograde metamorphic feature. The appearance of garnet in these gneisses is therefore considered not to affect the discussion below, which concerns the absence of reaction among aluminous pyroxenes, spinel, and plagioclase to give garnet and low-alumina pyroxenes. The apparent reaction of magnetite and plagioclase to yield garnet will not be considered here.

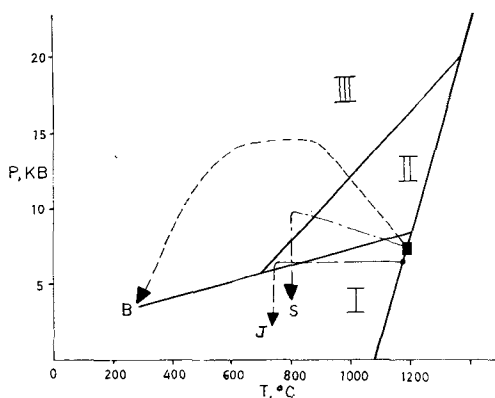
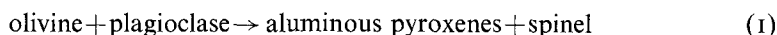


FIG. 3.  $P$ - $T$  diagram of subsolidus relations in the olivine-plagioclase system, after Kushiro and Yoder (1966), Green and Ringwood (1969), and Green and Hibberson (1970). Assemblages denoted by Roman numerals: I, oliv+plag; II, cpx+spin+plag; III, cpx+gnt+plag. Suggested  $P$ - $T$  histories are shown for rocks from Sognefjord (S) (Griffin, 1971*a*), Bergen (B) (Griffin, 1971*b*), and Jotunheimen (J).

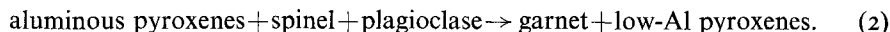
*Metamorphic History.* The sequence of phases in the reaction zone is analogous to that predicted from experimental studies on olivine-plagioclase systems. Kushiro and Yoder (1966), Green and Ringwood (1967), and Green and Hibberson (1970) have demonstrated that the low- $P$ , high- $T$  assemblage olivine+plagioclase reacts, with increasing  $P$  or decreasing  $T$ , to give the assemblage aluminous pyroxenes+spinel (fig. 3). Thus the apparent initial co-existence of olivine and plagioclase at the periodotite/gneiss contact limits the depth of solidification to less than 8 to 9 kb at magmatic temperatures ( $\sim 1200^\circ$ ). Isobaric cooling at moderate  $P$  would then be sufficient to produce the observed reaction rim; the distribution of the two pyroxenes in successive bands would simply reflect the necessary diffusion of different components in opposite directions.

The reaction:



has also been observed in anorthosites from Inner Sogn, at the western end of the Jotun nappe (Griffin, 1971*a*), from the Bergen Arcs (Griffin, 1971*b*), and from Lofoten

(Griffin and Heier, 1969). In all these localities, however, this reaction has been succeeded by a second reaction:



Why, then, has no garnet formed in the Jotunheimen rocks? Several possible explanations are considered below:

The  $P$ - $T$  curve for the appearance of garnet in olivine-plagioclase compositions is sensitive to Fe/Mg ratio of the olivine and the An content of the plagioclase (Green and Hibberson, 1970). The Jotunheimen and Bergen olivines, however, are essentially identical in composition ( $Fo_{77-78}$ ). The plagioclase is more sodic in the Jotunheimen rocks ( $An_{35}$  vs.  $An_{60}$ ) but this almost certainly reflects concentration of calcium into the clinopyroxene formed during reaction (1); similar low An values are observed near the coronas around olivine in the Bergen and Sognefjord rocks. A more likely composition for the original plagioclase is the  $An_{67}$  value observed in the breakdown symplectites. Thus it appears unlikely that compositional factors have suppressed the appearance of garnet in the Jotunheimen rocks.

Griffin (1971*b*) has observed that in the primary pyroxenes formed at  $P$  below that of reaction (1), and in the corona pyroxenes formed in reaction (1), the content of Tschermak's molecule should be proportional to  $P$  but relatively independent of  $T$  for a given bulk composition. This is suggested by the experimental work of Hays (1966) and Kushiro (1969). The 'primary' clinopyroxenes of the Bergen and Sogn anorthosites contain 20 to 25 % Ts, compared to 14 to 17 % for the analogous pyroxenes in the gneiss 58/63, even though all of these rocks originally contained the association olivine-clinopyroxene-spinel-plagioclase. Similarly, the corona clinopyroxene contains only 7 % Ts (14 % CaTs + Fe<sup>3+</sup>Ts) in Jotunheimen, compared to maxima of 20 % in Sogn and 25 % in Bergen.

There is thus good evidence in the pyroxene compositions that the Jotunheimen rocks have crystallized, and passed through reaction (1), at lower  $P$  than the Bergen and Sognefjord anorthosites.

If we consider an isobaric-cooling model, this  $P$  difference would also mean that reaction (2) would have been intersected at a lower  $T$ ; if this  $T$  were low enough it could be argued that kinetic factors alone could have prevented the growth of garnet. The  $\sim 20$  bars/degree slope of the line for reaction (2) (fig. 3) is not conclusively established (Green and Hibberson, 1970), but is favoured by the similar slopes of the 'eclogite' curve (Green and Ringwood, 1967), the  $Ab = Jd + Q$  curve, and others. If the convergence of reaction curves (1) and (2) is real, it sets a minimum value of around 700 °C for reaction (2) and limits the depth of isobaric cooling to  $> 6$  kb; this high  $T$  would seem to rule out purely kinetic factors as an explanation for the absence of garnet.

A more plausible explanation, suggested by the symplectitic breakdown of pyroxenes, is that the isobaric cooling history was somehow interrupted before reaction (2) was reached. Four types of pyroxene breakdown appear to be present:

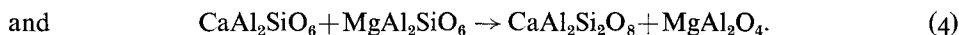
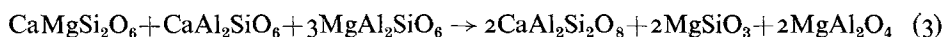
(a) The clinopyroxenes of the reaction zone and the peridotite break down to trains and patches of vermicular spinel-plagioclase-orthopyroxene intergrowth.

(b) Orthopyroxene in the reaction zone breaks down, mostly along grain boundaries, to plagioclase + spinel symplectites, and exsolves thin plates of spinel within the grains.

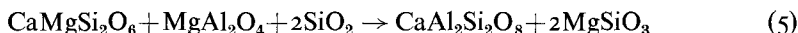
(c) Pyroxenes in the gneiss of sample 58/63 decompose to plagioclase, lower-Al clinopyroxene, and granules of low-Al orthopyroxene. Spinel is not present in the symplectites, and spinel grains in the gneiss appear to be corroded and are surrounded by rims of plagioclase.

(d) Pyroxenes in the gneiss JS23 break down to plagioclase, magnetite, and granules of low-Al pyroxenes (fig. 2).

The microprobe analyses of the primary phases and their breakdown products (tables I and II) indicate that the breakdowns involve the loss of the Ac and Ts components from the pyroxenes. A number of reactions, of varying plausibility, can be written to explain the symplectites and other products. Cases (a) and (b) might be explained by, respectively:

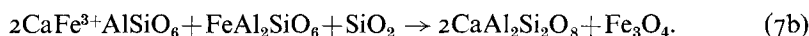
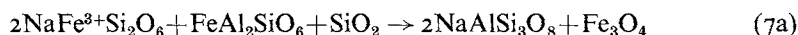


Reaction (3) might seem appropriate for case (c) as well, were it not for the apparent destruction, rather than production, of spinel. If the corrosion of the spinel is considered to be part of the pyroxene breakdown process then an outside source of silica is necessary. Possible reactions are:



The necessary silica might well be provided by simultaneously proceeding hydration reactions.

The appearance of magnetite as a reaction product in case (d) may result from reaction (3) coupled with the expulsion of acmite and  $\text{CaFeAlSiO}_6$  components from the pyroxene:



If oxidation is considered, then a possible reaction is



All of these reactions except (5) involve the expulsion of Tschermak's molecule from the clinopyroxene. The reactions involving addition of silica, or of oxygen, are not simply interpreted in terms of *P* and *T*. For example, Kushiro (1969) has pointed out that the Ts content of pyroxene will be lower in quartz-bearing assemblages than in an undersaturated assemblage at the same *P* and *T*. Thus the onset of hydration reactions, liberating silica, would tend to reduce the amount of Ts in the clinopyroxenes at a constant *T* and *P*. Reactions (3) and (4), however, can proceed isochemically, and are relatively unambiguous; Kushiro's (1969) experimental work strongly suggests that these two breakdown reactions proceed with a drop in pressure. The symplectitic



nature of the breakdown products suggests rapid reaction followed by chilling, and implies that the decompression may have taken place relatively rapidly and at high temperatures. Rapid cooling in the shallower environment could then preserve the breakdown products. If this was the case, then we can suggest that garnet is absent in the reaction zone because the rock was rapidly uplifted before it could cool through reaction (2). A similar interruption of the cooling process, but subsequent to reaction (2), was proposed for the Sognefjord anorthosites (Griffin, 1970a), in which corona garnet decomposed to opx-plag-spinel symplectites, and the cpx formed by reaction (1) broke down locally to opx-plagioclase-spinel symplectite.

*Tectonic implications.* Griffin (1971a) tentatively connected this decompression with the formation of the Jotun nappe, of which the Jotunheimen rocks are also a part. This interpretation implies that these rocks were still at depth, and hot, at the beginning of the Caledonian orogenic movements and then were upthrust. In other words, it implies that they are either very late Precambrian or early Caledonian intrusives, unless an unreasonably slow cooling rate is proposed.

Several points, however, argue strongly against this interpretation. The only available radiometric age is a single-rock Rb/Sr age of  $1.55 \times 10^6$  yr. on a granite of the Jotun nappe underlying the Hardanger glacier (Priem, 1968), but it is generally accepted that the anorthosites and associated rocks are all Precambrian. In the Bergen area it seems probable that there is a large age difference between the low-grade Cambro-Silurian supracrustal rocks and the high-grade anorthosites and gneisses that underlie them (Griffin, 1971b). More concretely, there is firm evidence that the Eocambrian sediments of the Valdres sparagmite were deposited directly upon the Jotun rocks and thus that the Jotun rocks were *unroofed* by Eocambrian time (Loeschke and Nickelsen, 1968).

If these time relations are correct, we must conclude that the coronas and the decompression textures of the Sogn and Jotunheimen rocks reflect only their Precambrian histories, and say nothing about the formation of the Caledonian nappe structures. In this case it would be merely a remarkable coincidence that these decompression features are found only within the nappe structure; such textures are lacking in Bergen, where there is more evidence that the anorthosites and the surrounding gneisses are part of a single, slowly uplifted terrane (Griffin, 1971b).

The element of coincidence may be removed by hypothesizing that the Jotun nappe rocks, which must have crystallized at middle to lower crustal levels, were thrust upward into the upper crust in Precambrian time and were subsequently unroofed, and that the marginal thrusting now visible resulted from remobilization during the Caledonian orogeny. Geophysical data (Ramberg and Grønlie, 1969; Smithson and Ramberg, 1970) show a thick wedge of high-density rocks underlying the Upper Jotun Nappe, and allow interpretation of the Jotun rocks as upthrust sub-Conrad material, in contrast to the classic idea that the nappes are thin flat-lying sheets derived from a distant root zone. Smithson and Ramberg (1970) have suggested that the root of the nappe lies under the Jotunheimen, and that the area is generally similar to the Alpine Ivrea zone. If we accept a Precambrian decompression event as suggested

by the coronas, we can speculate that this Ivrea-type structure was the locus of strong upward movement of lower-crustal material already in Precambrian time, and was reactivated in the Caledonian orogeny. This later portion of the rocks' history would be at low temperatures and would not be recorded in the coronas except as the secondary hydration reactions associated with shearing.

Whichever interpretation is correct, we may summarize the early history of the Jotunheimen rocks as follows:

Solidification at  $P \approx 8$  kb, and probably closer to 6 kb by comparison with the Bergen and Sogn anorthosites.

Cooling to 800–900 °C, passing through reaction (1).

Rapid uplift, terminating the high- $P$  cooling, preventing the formation of garnet and resulting in decomposition of the higher- $P$  aluminous pyroxenes.

Rapid cooling at relatively shallow depths, preserving the symplectite mineralogy.

It seems possible now to suggest a general picture of the  $P$ – $T$  relations of the central Norwegian anorthosites. The eastern end of the thrust mass in Jotunheimen represents a relatively shallow level compared to the western end (Sognefjord). These two areas may have cooled to approximately similar  $T$  (800–900°?) before having rapidly uplifted; the timing of this uplift and its significance in orogenic terms are still not clear. The westernmost exposures of these rocks, the Bergen arc anorthosites, were apparently intruded at depths comparable to the Sognefjord anorthosites. However, they were buried to greater depths during cooling, and cooled to much lower temperatures (500°?). There is no sign of rapid decompression in these rocks; on the contrary, slow uplift at relatively low  $T$  is implied. It is tempting to speculate that all of these rocks were intruded during one period at various depths, and that orogenic movements subsequently depressed the Bergen area while elevating the Jotun-nappe rocks to upper-crustal levels.

*Acknowledgements.* The material on which this study is based was supplied by Dr. M. H. Battey, University of Newcastle upon Tyne, who has been engaged for a number of years on mapping parts of Jotunheimen. He has also collaborated by providing some petrographic details and the drawing for fig. 2. His descriptions of the field relationships are referred to above.

This work was supported by research grants to Prof. K. S. Heier from Norges Almenvitenskapelige Forskningsråd and by a Post-Doctoral Fellowship (WLG) from Norges Teknisk Naturvitenskapelige Forskningsråd. I thank I. Bryhni, I. Ramberg, and S. Smithson for reviewing the manuscript and for stimulating discussions. B. Tøtdal gave much assistance during the microprobe work.

#### REFERENCES

- BATTEY (M. H.), 1960. *Rept. XXI Internat. Geol. Congress*, pt. 13, 198.  
 — 1965. *Min. Mag.* **34**, 35.  
 GOLDSCHMIDT (V. M.), 1916. *Videnskaps Skrifter, Oslo. I. Mat.-naturv. Kl, no. 2*.  
 GREEN (D. H.) and HIBBERSON (W.), 1970. *Lithos*, **3**, 296.  
 — and RINGWOOD (A. E.), 1967. *Contr. Min. Petr.* **15**, 103.  
 GRIFFIN (W. L.), 1971a. *Journ. Petrology* (in press).  
 — 1971b. *Mem. Geol. Soc. Amer.* (in press).  
 — and HEIER (K. S.), 1969. *Contr. Min. Petr.* **23**, 89.

- HAYS (J. F.), 1966. *Carnegie Inst. Wash. Yearbook* **65**, 234.  
KUSHIRO (I.), 1969. *Min. Soc. Amer. Spec. Publ.* **2**, 179.  
— and YODER (H. S.), 1966. *Journ. Petrology* **7**, 337.  
KVALE (A.), 1960. *XXI Int. Geol. Congr., Guide to Excurs. A7 and C4*.  
LOESCHKE (J.) and NICKELSEN (R. P.), 1968. *Neues. Jahrb. Geol. Paläont., Abh.* **131**, 337.  
PRIEM (H. N. A.), 1968. *Z.W.V. Laborat. voor Isotope Geol. Progress Report*.  
RAMBERG (I. B.) and GRØNLIE (G.), 1969. *Bull. Geofis. Theor. Applic.* **11**, 219.  
SMITHSON (S. B.) and RAMBERG (I. B.), 1970. *Bull. Geol. Soc. Amer.* **81**, 1571.

[Manuscript received 26 November 1970.]